Available online at www.sciencedirect.com
ScienceDirect
Solid State Communications 142 (2007) 421–424
solid state communications
www.elsevier.com/locate/ssc

Fast-track communication

Superconducting transition parameters in aluminum–lithium alloys (0–10 at.% Li)

M.N. Ou[a,b], T.J. Yang[a], B.J. Chen[b], Y.Y. Chen[b], J.C. Ho[c,*]

[a] *Department of Electrophysics, National Chiao Tung University, Hsinchu, Taiwan*
[b] *Institute of Physics, Academia Sinica, Taipei, Taiwan*
[c] *Department of Physics, Wichita State University, Wichita, KS, USA*

Received 12 March 2007; accepted 25 March 2007 by A.H. MacDonald
Available online 31 March 2007

Abstract

The superconducting transition temperatures T_c of face-centered cubic Al_{1-x}–Li_x alloys (x = 0–0.10) exhibit a minimum near $x = 0.03$ (3 at.% Li). The McMillan strong-coupling T_c equation yields a similar trend of the electron–phonon coupling constant λ. Meanwhile, the density of states at the Fermi level $N(0)$ decreases monotonically with increasing x. It appears that T_c drops initially due to a reduced $N(0)$, which is then overtaken by alloying-enhanced factors of phonon or electron–phonon interaction.

PACS: 74.62.Bf; 74.70.Ad

Keywords: A. Superconductors; D. Electron–phonon interactions

1. Introduction

Extensive research on cuprate superconductors has revealed their many unique characteristics, but the detailed mechanism leading to the critical phenomenon remains elusive. For traditional superconductors, the BCS theory [1] provides an elegant description of the superconducting electron pair formation induced by attractive electron–phonon interaction. The superconducting transition temperature is given by the expression

$$kT_c = 1.14\langle\hbar\omega\rangle \exp[-1/N(0)V], \tag{1}$$

where k is the Boltzmann constant, $\langle\hbar\omega\rangle$ the average energy of phonons which scatter electrons at Fermi level, $N(0)$ the electronic density of states at the Fermi level, and V the parameter measuring the difference between Coulomb repulsion and phonon-induced attraction of electrons close to the Fermi level. Then, building on earlier work of Eliashberg [2], McMillan [3] extended the BCS equation to take into account the effective Coulomb repulsion strength μ^* and the electron–phonon spectral function $\alpha^2(\omega)F(\omega)$. From the latter, a dimensionless electron–phonon interaction parameter λ is introduced, yielding the more generalized strong-coupling formula,

$$T_c = \frac{\theta_D}{1.45} \exp\left[-\frac{1.04(1+\lambda)}{\lambda - \mu^*(1+0.62\lambda)}\right], \tag{2}$$

with θ_D being the Debye temperature. While μ^* has a limited range, λ varies appreciably from 0.23 for Be (T_c = 0.026 K) to 1.75 for Nb_3Sn (T_c = 17.8 K) [4,5].

In practice, T_c of any given material still relies on experimental determination. By rearranging Eq. (2) to

$$\lambda = \frac{1.04 + \mu^* \ln(\theta_D/1.45T_c)}{(1-0.62\mu^*)\ln(\theta_D/1.45T_c) - 1.04}, \tag{3}$$

experimentally derived T_c and θ_D are often used to calculate λ. A brief description and summarized λ values can be found in a recent review article by Allen [5].

The sp-metal aluminum has a relatively low λ of 0.38. This work on Al–Li is for the purpose of adding more information to

* Corresponding author. Tel.: +1 316 978 3992.
E-mail address: james.ho@wichita.edu (J.C. Ho).

0038-1098/$ - see front matter © 2007 Elsevier Ltd. All rights reserved.
doi:10.1016/j.ssc.2007.03.039

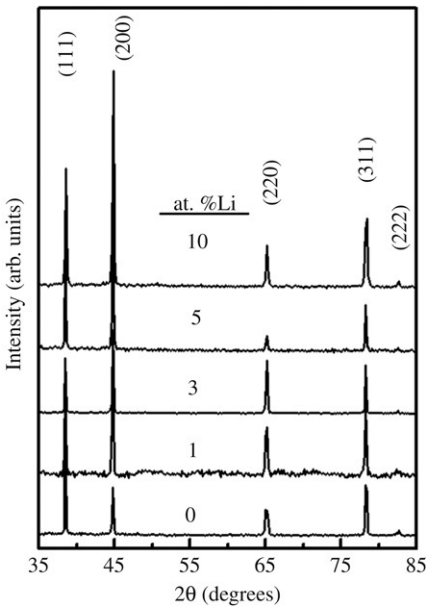

Fig. 1. X-ray diffraction patterns confirming the fcc structure in all samples.

the alloying effect on λ, which can be further analyzed as [3]

$$\lambda = N(0)\langle \mathscr{I}^2 \rangle / M\langle \omega^2 \rangle, \tag{4}$$

where $\langle \mathscr{I}^2 \rangle$ and $\langle \omega^2 \rangle$ are the mean square electron–phonon matrix element and phonon frequency, respectively, and M is the atomic mass. Based on calorimetric and tunneling data, such a delineation procedure has been made on binary Tl–Pb and Pb–Bi and ternary Tl–Pb–Bi alloys [6,7].

2. Experiment and results

Aluminum–lithium-base alloys, with additions of other elements such as copper and magnesium, are among the commercially available high-strength and light-weight structural materials. The phase diagram of the Al–Li binary system has been well established [8]. Four face-centered cubic α-phase Al_{1-x}–Li_x samples having nominal compositions of 1, 3, 5, and 10 at.% Li (x = 0.01, 0.03, 0.05 and 0.10), respectively, were prepared by pyrosynthesis. For each composition, a weighted mixture of Al (99.9995% purity) and Li (99.9% purity) was contained in a graphite crucible inside a bell jar evacuated and refilled with argon. After being melted above 750 °C, the molten charge was poured into a 0.5 inch diameter steel mold. Knowing that the Li solubility is low at ambient temperature but 10 at.% at 500 °C and 14 at.% at the 600 °C-eutectic [8], the product was homogenized by annealing at 500 °C, followed by ice-brine quenching. Practically no weight loss occurred during the process. X-ray diffraction patterns, from a Phillips MPD diffractometer with Cu $K\alpha_1$ radiation, shown in Fig. 1, confirm the fcc-phase structure. The lattice constant decreases monotonically with increasing Li content from approximately 4.052 Å for pure aluminum, which agrees with the literature value, to 4.030 Å at 10 at.% Li.

Calorimetric measurements between 2 and 10 K on these samples have been made and reported earlier [9].

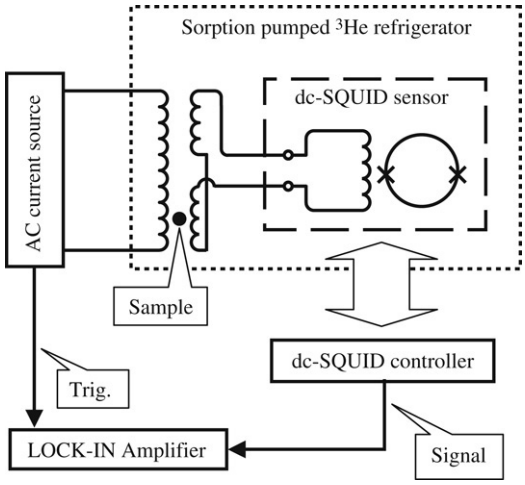

Fig. 2. Sketch of ac-susceptibility measuring system.

No superconductivity was detected then as expected, since aluminum has a T_c value near 1 K. In this work magnetic measurements were employed. Considering the relatively low critical field H_c = 105 G for aluminum, conventional dc-susceptibility measurements with an applied field $H \geq$ 10 G would cause transition broadening and T_c-shifting. To overcome these complications, a low-temperature and low-field ac-susceptibility setup was constructed, as shown in the sketch in Fig. 2. A commercial dc-SQUID sensor and homemade signal pickup coils are mounted on the sorption-pumped ^{3}He refrigerator system having a base temperature close to 0.4 K. Along with two self-compensating secondary coils having the sample inserted into one of them, the primary coil is connected to an ac-current source. At 15.97 Hz, the current-induced magnetic field has a sine-wave profile of amplitude ∼20 mG.

The temperature dependence of the real part of the diamagnetic signals χ'_{ac} in Fig. 3 clearly identifies the superconducting transitions. For pure aluminum ($x = 0$), T_c = 1.16 K (mid-point of the transition) agrees with the literature value [10]. The narrow transition widths ($\Delta T_c \sim 0.2$ K, based on 20% and 80% of normal-state χ'_{ac}) further confirm the phase purity in the alloys. Only one broader transition ($\Delta T_c \sim 0.5$ K) occurs at 10 at.% Li, which may reflect a less-than-sufficient quenching rate near the fcc-phase boundary. Even so, this would not present any problem in data analysis below.

3. Discussions

In the previous report [9] of calorimetric measurements on the same samples, each set of low-temperature specific heat data was analyzed as the summation of an electronic (γT) and a lattice (βT^3) term, both varying monotonically with increasing x. The Debye model yields θ_D from the lattice specific heat coefficient β. The electronic specific heat coefficient γ can be used to calculate $N(0)$,

$$\gamma = (2\pi^2/3)k^2(1+\lambda)N(0) \tag{5}$$

provided that λ is available.

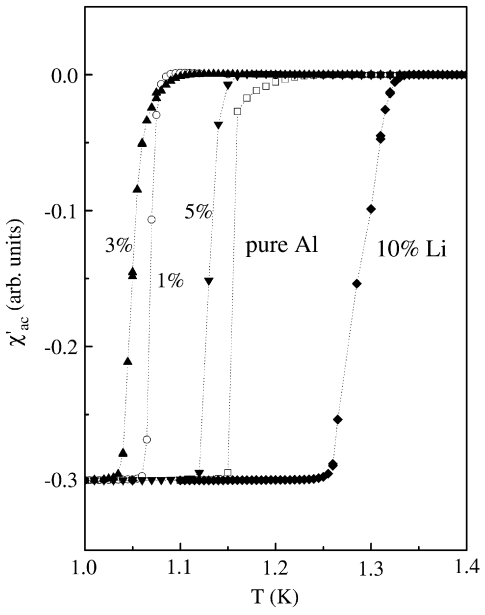

Fig. 3. Magnetic susceptibility data showing superconducting transitions.

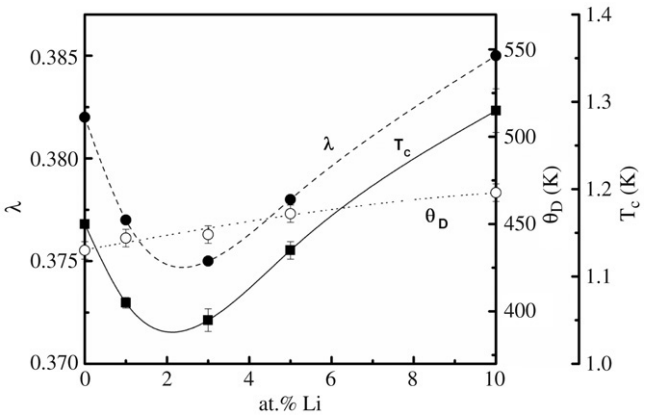

Fig. 4. Li-content dependence of λ calculated from experimentally derived T_c and θ_D.

As shown in Fig. 4, T_c undergoes an initial drop of about 10%, reaching a minimum near 3 at.% Li, then increases by almost 25% at 10 at.% Li. Apart from the relatively slow varying θ_D, one needs to know μ^* in order to derive λ from Eq. (3). According to the review article by Allen [5], knowledge of μ^* is primitive and it is assumed to be 0.10–0.13. For the lower T_c superconductors being considered here, $\mu^* = 0.10$ would be justifiable. The λ values thus obtained are included in Fig. 4. They show also a minimum near 3 at.% Li. Their determination leads further to the calculated density of states $N(0)$ from Eq. (5), which is among the most important electronic properties. Along with the calorimetrically derived θ_D and γ, the superconductivity-related parameters T_c, λ, and $N(0)$ thus obtained are listed in Table 1.

The exact value of λ certainly relies on the selection of μ^*. More important to this study, however, is to elucidate the alloying or Li-content effect on T_c. For this purpose, an additional test was made to ascertain the Li-content dependence

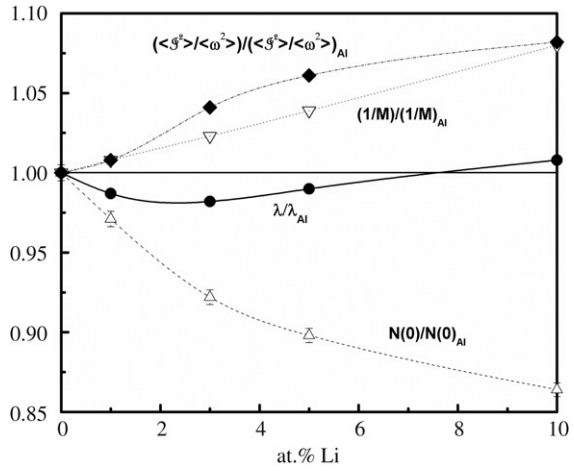

Fig. 5. Li-content dependence of normalized parameters in Eq. (4), relative to pure Al. The error bar of $N(0)$ reflects the uncertainty in calorimetrically determined γ.

Table 1
Superconducting transition temperature and related parameters in fcc Al_xLi_{1-x}

x	T_c (K)	θ_D[a] (K)	μ^*[b]	λ	γ[a] (mJ/mol K^2)	$N(0)$ (eV^{-1})
0	1.16	435	0.10	0.382	1.34	0.206
0.01	1.07	442	0.10	0.377	1.30	0.200
0.03	1.05	444	0.10	0.375	1.23	0.190
0.05	1.13	456	0.10	0.378	1.20	0.185
0.10	1.29	468	0.10	0.385	1.16	0.178

[a] From Ref. [8].
[b] Assumed value after Ref. [5].

Table 2
Variation of λ on Li content, based on three differently assigned constant μ^* values

x	$\mu^* = 0.09$	$\mu^* = 0.10$	$\mu^* = 0.11$
0	0.366	0.382	0.399
0.01	0.360	0.377	0.393
0.03	0.359	0.375	0.392
0.05	0.362	0.378	0.394
0.10	0.368	0.385	0.401

of λ. This was done by varying μ^* to different constant values of 0.09 and 0.11, respectively. As clearly shown in Table 2, a minimum in λ invariably prevails near $x = 0.03$ (3 at.% Li). Consequently, in the further analysis based on Eq. (4) below, $\mu^* = 0.10$ for all samples and their corresponding λ values are used.

With reference to pure aluminum, the normalized values of λ, $N(0)$, $1/M$ and calculated ratio of $\langle\mathscr{I}^2\rangle/\langle\omega^2\rangle$ from Eq. (4) as listed in Table 3 are shown in Fig. 5. Tunneling data, if available, could help delineate the $\langle\mathscr{I}^2\rangle/\langle\omega^2\rangle$ ratio [7]. Without such, though, one can still conclude that T_c drops initially due to a reduced $N(0)$, which is then overtaken by alloying-enhanced factors of phonon or electron–phonon interaction, resulting in the observed T_c minimum near $x = 0.03$ (3 at.% Li).

Table 3
Normalized parameters in Eq. (4) based on $\mu^* = 0.10$, relative to pure Al

x	λ/λ_{Al}	$N(0)/N(0)_{Al}$	$(1/M)/(1/M)_{Al}$	$(\langle\mathscr{I}^2\rangle/\langle\omega^2\rangle)/(\langle\mathscr{I}^2\rangle/\langle\omega^2\rangle)_{Al}$
0	1.000	1.000	1.000	1.000
0.01	0.987	0.971	1.008	1.008
0.03	0.982	0.922	1.023	1.041
0.05	0.990	0.898	1.039	1.061
0.10	1.008	0.864	1.080	1.082

Acknowledgment

The work at Academia Sinica was supported by the National Research Council, the Republic of China, under Grant No. NSC 94-2112-M-001-044.

References

[1] J. Bardeen, L.N. Cooper, J.R. Schrieffer, Phys. Rev. 108 (1957) 1175.
[2] G.M. Eliashberg, Soviet Phys. JETP 11 (1960) 696.
[3] W.L. McMillan, Phys. Rev. 167 (1968) 331.
[4] P.B. Allen, R.C. Dynes, Phys. Rev. B 12 (1975) 905.
[5] P.B. Allen, in: C.P. Poole Jr. (Ed.), Handbook of Superconductivity, Academic Press, New York, 2000, p. 478.
[6] R.C. Dynes, J.M. Rowell, Phys. Rev. B 11 (1975) 1884.
[7] F. Hermans, J.C. Ho, J. Boyer, N.E. Phillips, J. de Physique C6 (1978) 477.
[8] A.J. McAlister, Bull. Alloy Phase Diagrams 3 (1982) 177.
[9] C.R. Wang, S. Neeleshwar, Y.Y. Chen, J.C. Ho, J. Appl. Phys. 94 (2003) 7938.
[10] N.E. Phillips, Phys. Rev. 114 (1959) 676.